WARWICK
THE UNIVERSITY OF WARWICK

Manuscript version: Author's Accepted Manuscript
The version presented in WRAP is the author's accepted manuscript and may differ from the published version or Version of Record.

Persistent WRAP URL:
http://wrap.warwick.ac.uk/141832

How to cite:
Please refer to published version for the most recent bibliographic citation information. If a published version is known of, the repository item page linked to above, will contain details on accessing it.

Copyright and reuse:
The Warwick Research Archive Portal (WRAP) makes this work by researchers of the University of Warwick available open access under the following conditions.

Copyright © and all moral rights to the version of the paper presented here belong to the individual author(s) and/or other copyright owners. To the extent reasonable and practicable the material made available in WRAP has been checked for eligibility before being made available.

Copies of full items can be used for personal research or study, educational, or not-for-profit purposes without prior permission or charge. Provided that the authors, title and full bibliographic details are credited, a hyperlink and/or URL is given for the original metadata page and the content is not changed in any way.

Publisher's statement:
Please refer to the repository item page, publisher's statement section, for further information.

For more information, please contact the WRAP Team at: wrap@warwick.ac.uk.

Joint Location and Transmit Power Optimization for NOMA-UAV Networks via Updating Decoding Order

***Abstract*—Unmanned aerial vehicle (UAV) can be combined with non-orthogonal multiple access (NOMA) to achieve better performance. However, jointly optimizing the location, transmit power and decoding order for NOMA-UAV networks remains difficult, due to the change of decoding order as a result of UAV mobility. In this letter, a low-complexity scheme is proposed to maximize the sum rate of NOMA-UAV networks via updating decoding order, which can be decomposed into two steps. First, the joint location and power optimization can be divided into two non-convex sub-problems, which are further approximated via successive convex optimization. Then, the decoding order is updated according to the optimized UAV location. An iterative algorithm is proposed to execute the two steps alternately. In addition, the asymptotic performance is analyzed. Simulation results demonstrate the effectiveness of the proposed scheme.**

***Index Terms*—NOMA, power and location optimization, successive interference cancellation, UAV.**

I. INTRODUCTION

Recently, unmanned aerial vehicles (UAVs) have been widely used as carrying platforms of base stations in wireless communications [1], [2]. Many recent studies have been dedicated to UAV communications [3]–[7]. In [3], the joint optimization of trajectory and transmit power was studied by Wu *et al*. to maximize the sum rate in multi-UAV networks. Yang *et al.* studied UAV energy tradeoff for the data collection in UAV networks via trajectory optimization in [4]. Zhao *et al.* [5] proposed a novel channel tracking scheme for UAV mmWave multi-antenna systems. In [6], Gong *et al.* considered a UAV-assisted cellular network, applying the superimposed training sequence with imperfect channel statistics. UAV-aided jamming for secure communication with unknown location of the eavesdropper was investigated in [7] by Nnamani *et al*.

Manuscript received August 10, 2020; revised September 4, 2020; accepted September 7, 2020. The work was supported by the National Natural Science Foundation of China (NSFC) under Grant 61871065 and 61971194, and also supported by the project "The Verification Platform of Multi-tier Coverage Communication Network for Oceans (LZC0020)". The associate editor coordinating the review of this paper and approving it for publication was M. R. A. Khandaker. *(Corresponding author: Nan Zhao.)*

On the other hand, to improve the spectrum efficiency, non-orthogonal multiple access (NOMA) is emerging as a crucial technique for future wireless networks [8]–[10]. In [8], Chen *et al*. have proved that NOMA has a better performance than orthogonal multiple access (OMA). A resource allocation algorithm for NOMA networks was proposed by Chang *et al*. to improve the secrecy energy efficiency [9]. In [10], Lei *et al*. proposed a max-min transmit antenna selection scheme for NOMA systems with secrecy outage performance analyzed.

Due to their advantages, it becomes natural to integrate UAV and NOMA for enhancing the performance, and some fundamental works have been done in [11], [12]. Liu *et al*. set up a general framework for NOMA-UAV networks in [11]. Mei and Zhang proposed a cooperative NOMA scheme for cellular-connected UAV networks in [12]. Recently, plenty of research on resource allocation of NOMA-UAV network has been conducted [13]–[17]. In [13], Tang *et al*. proposed a UAV placement scheme to maximize the number of users in a NOMA-UAV network. A joint placement and power optimization scheme was proposed by Liu *et al*. for NOMA-UAV networks in [14]. The joint optimization of altitude and beamwidth was considered in a NOMA-UAV network by Nasir *et al*. in [15]. Liu *et al*. proposed a distributed NOMA-UAV scheme to assist emergency communications [16]. Wang *et al*. [17] proposed a UAV-aided NOMA scheme with secure simultaneous wireless information and power transfer. Resource allocation for optimizing the energy efficiency in NOMA-UAV network was introduced in [18], [19].

Motivated by above works, we focus on the system design for NOMA-UAV networks. The location and transmit power of UAV are jointly optimized to maximize the sum rate. Different from above works with fixed decoding order, we propose an iterative algorithm to update the current decoding order in the ascending order of channel gains after each iteration. Numerical results show that the proposed scheme can effectively improve the performance of NOMA-UAV networks.

II. SYSTEM MODEL AND PROBLEM FORMULATION

A. System Model

Consider a NOMA-UAV network with one UAV and K ground users. All are equipped with a single antenna. Define

U_i as the ith user, $i \in \mathcal{K} \triangleq \{1, 2, \ldots, K\}$. The superimposed information is transmitted from the UAV to the users via NOMA. The received signal at U_i is given by

$$s_i = h_i \sum_{j=1}^{K} z_j + n_i, \;\; i \in \mathcal{K}, \tag{1}$$

where h_i represents the channel coefficient from the UAV to U_i, and n_i denotes the additive white Gaussian noise (AWGN) at U_i. z_j is the message for U_j with $|z_j|^2 = a_j P_{sum} = P_j$, where P_{sum} is the sum transmit power of UAV, a_j is the power coefficient of U_j, and P_j is the transmit power for U_j.

Assume that the horizontal coordinates of U_i is denoted as $\mathbf{q}_i = [x_i, y_i]^{\mathrm{T}} \in \mathbb{R}^{2\times 1}$. The UAV hovers at a fixed altitude H and its horizontal coordinate is $\mathbf{L} = [X, Y]^{\mathrm{T}} \in \mathbb{R}^{2\times 1}$. The distance between the UAV and U_i can be expressed as

$$d_i = \sqrt{H^2 + \|\mathbf{q}_i - \mathbf{L}\|^2}. \tag{2}$$

The probability of UAV-to-ground links dominated by line-of-sight (LoS) can be expressed as

$$\mathbf{P}_i^{\mathrm{LoS}} = \frac{1}{1 + a_0 \exp(-b_0(\theta_i - a_0))}, \tag{3}$$

where a_0 and b_0 denote the environment constants. $\theta_i = \arcsin\left(\frac{H}{d_i}\right)$ represents the elevation angle between the UAV and U_i. According to an extensive survey for UAV channel modeling [20], when the UAV is located high enough (e.g., 120m), the LoS probability is approximate to 1. Thus, the channel from the UAV to U_i can be denoted as

$$h_i = \sqrt{\rho_0 d_i^{-2}} = \sqrt{\frac{\rho_0}{H^2 + \|\mathbf{q}_i - \mathbf{L}\|^2}}, \tag{4}$$

where ρ_0 denotes the reference channel gain at the unit distance.

According to NOMA, the successive interference cancellation (SIC) is applied for users to receive their own messages, and users with low channel gains are compensated by high power allocation ratios. Therefore, according to the distance from the UAV to users, we assume $|h_1|^2 \geq \cdots \geq |h_i|^2 \geq \cdots \geq |h_K|^2 > 0$ with $0 < a_1 \leq \cdots \leq a_i \leq \cdots \leq a_K$. U_i needs to decode the messages from U_{i+1} to U_K and removes them from the superposed signal. Then, we can express the signal-to-interference-plus-noise-ratio (SINR) for U_i $(2 \leq i \leq K)$ as

$$\mathrm{SINR}_i = \frac{|h_i|^2 P_i}{|h_i|^2 \sum\limits_{k=1}^{i-1} P_k + \sigma^2} = \frac{P_i}{\sum\limits_{k=1}^{i-1} P_k + \dfrac{\sigma^2}{|h_i|^2}}, \tag{5}$$

where σ^2 is the power of AWGN at user receivers. When $i = 1$, the received SINR can be calculated by

$$\mathrm{SINR}_1 = \frac{P_1 |h_1|^2}{\sigma^2}. \tag{6}$$

Thus, the transmission rate for U_i can be denoted as

$$R_i = \log_2\left(1 + \mathrm{SINR}_i\right), \;\; i \in \mathcal{K}. \tag{7}$$

We assume γ_i denotes the SINR threshold of U_i, which can be expressed as

$$\mathrm{SINR}_i \geq \gamma_i, \;\; i \in \mathcal{K}. \tag{8}$$

Accordingly, the rate threshold of U_i is obtained from (8) as

$$\eta_i = \log_2(1 + \gamma_i), \;\; i \in \mathcal{K}. \tag{9}$$

B. Problem Formulation

Define $\mathbf{P} = \{P_i, i \in \mathcal{K}\}$. To maximize the sum rate of ground users via jointly optimizing $\mathbf{L}$ and $\mathbf{P}$ based on (7) and (8), the optimization problem can be formulated as

$$\max_{\mathbf{L},\mathbf{P}} \; \sum_{i\in\mathcal{K}} \log_2\left(1 + \; \mathrm{SINR}_i\right) \tag{10a}$$
$$s.t. \;\; \mathrm{SINR}_i \geq \gamma_i, \tag{10b}$$
$$0 < P_1 \leq \cdots \leq P_i \leq \cdots \leq P_K, \tag{10c}$$
$$\sum_{i=1}^{K} P_i \leq P_{sum}. \tag{10d}$$

Combining (5), (6) and (7), the problem (10) can be rewritten as

$$\max_{\mathbf{L},\mathbf{P}} \; \sum_{i\in\mathcal{K}} \log_2\left(1 + \; \mathrm{SINR}_i\right) \tag{11a}$$
$$s.t. \;\; \frac{P_i}{\sum\limits_{k=1}^{i-1} P_k + \dfrac{\sigma^2}{|h_i|^2}} \geq \gamma_i, \forall i \in \mathcal{K}\backslash\{1\}, \tag{11b}$$
$$P_1 |h_1|^2 / \sigma^2 \geq \gamma_1, \tag{11c}$$
$$0 < P_1 \leq \cdots \leq P_i \leq \cdots \leq P_K, \tag{11d}$$
$$\sum_{i=1}^{K} P_i \leq P_{sum}. \tag{11e}$$

In (11), the constraints (11b) and (11c) are non-convex with respect to $\mathbf{L}$ and $\mathbf{P}$. Thus, approximation will be used in the next section.

Different from the fixed SIC order [14], the decoding order is updated after each iteration according the ranking of channel gains in this letter, with the stronger user decoded later.

III. Iterative Algorithm for the Optimization

The problem (11) is difficult to solve due to its non-convexity. Thus, we propose a scheme to optimize the location and power alternately via successive convex optimization.

A. Transmit Power Optimization

First, we fix the UAV location and (11) becomes

$$\max_{\mathbf{P}} \; \sum_{i\in\mathcal{K}} \log_2\left(1 + \; \mathrm{SINR}_i\right) \tag{12a}$$
$$s.t. \;\; \frac{P_i}{\sum\limits_{k=1}^{i-1} P_k + \dfrac{\sigma^2}{|h_i|^2}} \geq \gamma_i, i \in \mathcal{K}\backslash\{1\}, \tag{12b}$$
$$(11\mathrm{c}), (11\mathrm{d}), (11\mathrm{e}). \tag{12c}$$

(12c) is convex. (12b) is non-convex and its left-hand-side can be replaced by R_i. Thus, it can be changed into two concave functions with respect to $\mathbf{P}$ as

$$\begin{aligned} R_i &= \log_2\left(1 + \mathrm{SINR}_i\right) \\ &= \log_2\left(1 + \frac{|h_i|^2 P_i}{|h_i|^2 \sum_{k=1}^{i-1} P_k + \sigma^2}\right) \\ &= \log_2\left(|h_i|^2 \sum_{k=1}^{i} P_k + \sigma^2\right) - \log_2\left(|h_i|^2 \sum_{k=1}^{i-1} P_k + \sigma^2\right). \end{aligned} \tag{13}$$

We need to approximate the second concave function via the first-order Taylor expansion at a specific point to obtain its global upper-bound. Define the transmit power in the rth iteration and the second concave function as $\mathbf{P}^r$ and $\bar{R}_i$, respectively, and we have

$$\begin{aligned}\bar{R}_i &= \log_2\left(|h_i|^2 \sum\nolimits_{k=1}^{i-1} P_k + \sigma^2\right)\\ &\le \sum\nolimits_{k=1}^{i-1} A_i^r\left(P_k - P_k^r\right) + B_i^r \triangleq \bar{R}_i^{[ub]},\end{aligned} \tag{14}$$

where A_i^r and B_i^r can be calculated as

$$A_i^r = \frac{|h_i|^2 \log_2(e)}{|h_i|^2 \sum_{l=1}^{i-1} P_l^r + \sigma^2}, \tag{15}$$

$$B_i^r = \log_2\left(|h_i|^2 \sum\nolimits_{k=1}^{i-1} P_k^r + \sigma^2\right). \tag{16}$$

Therefore, (12) becomes convex as

$$\max_{\mathbf{P}} \ \sum\nolimits_{i\in\mathcal{K}} \log_2\left(1 + \ \mathrm{SINR}_i\right) \tag{17a}$$

$$s.t.\ \ \log_2\left(|h_i|^2 \sum_{k=1}^{i} P_k + \sigma^2\right) - \bar{R}_i^{[ub]} \ge \eta_i, \forall i \in \mathcal{K}\backslash\{1\}, \tag{17b}$$

$$(11\mathrm{c}), (11\mathrm{d}), (11\mathrm{e}), \tag{17c}$$

which is convex and can be solved by CVX.

B. Location Optimization

Then, we fix the transmit power to transform (11) into

$$\max_{\mathbf{L}} \ \sum\nolimits_{i\in\mathcal{K}} \log_2\left(1 + \ \mathrm{SINR}_i\right) \tag{18a}$$

$$s.t. \ \begin{cases} \dfrac{\dfrac{\rho_0}{H^2 + \|\mathbf{q}_i - \mathbf{L}\|^2} P_i}{\dfrac{\rho_0}{H^2 + \|\mathbf{q}_i - \mathbf{L}\|^2} \sum_{k=1}^{i-1} P_k + \sigma^2} \ge \gamma_i, \\ \forall i \in \mathcal{K}\backslash\{1\}, \end{cases} \tag{18b}$$

$$\frac{P_1 \rho_0}{\sigma^2 \left(H^2 + \|\mathbf{q}_1 - \mathbf{L}\|^2\right)} \ge \gamma_1. \tag{18c}$$

The constraints (18b) and (18c) are non-convex with respect to $\mathbf{L}$. For (18b), it can be split into two convex functions with respect to $\|\mathbf{q}_i - \mathbf{L}\|^2$ as

$$\begin{aligned} R_i =& \log_2\left(1 + \mathrm{SINR}_i\right) \\ =& \log_2\left(1 + \frac{\dfrac{\rho_0}{H^2 + \|\mathbf{q}_i - \mathbf{L}\|^2} P_i}{\dfrac{\rho_0}{H^2 + \|\mathbf{q}_i - \mathbf{L}\|^2} \sum_{k=1}^{i-1} P_k + \sigma^2}\right) = \tilde{R}_i - \hat{R}_i, \end{aligned} \tag{19}$$

where

$$\tilde{R}_i = \log_2\left(\frac{\rho_0}{H^2 + \|\mathbf{q}_i - \mathbf{L}\|^2} \sum\nolimits_{k=1}^{i} P_k + \sigma^2\right), \tag{20}$$

$$\hat{R}_i = \log_2\left(\frac{\rho_0}{H^2 + \|\mathbf{q}_i - \mathbf{L}\|^2} \sum\nolimits_{k=1}^{i-1} P_k + \sigma^2\right). \tag{21}$$

Notice that $\tilde{R}_i$ is neither concave nor convex with respect to $\mathbf{L}$. Thus, we define the local point $\mathbf{L}^r$ in the rth iteration and derive the lower-bounded expression of $\tilde{R}_i$ via the first-order Taylor expansion as

$$\begin{aligned} \tilde{R}_i &= \log_2\left(\frac{\rho_0}{H^2 + \|\mathbf{q}_i - \mathbf{L}\|^2} \sum_{k=1}^{i} P_k + \sigma^2\right) \\ &\ge \sum_{k=1}^{i} -C_i^r\left(\|\mathbf{q}_i - \mathbf{L}\|^2 - \|\mathbf{q}_i - \mathbf{L}^r\|^2\right) + D_i^r \triangleq \tilde{R}_i^{[lb]}, \end{aligned} \tag{22}$$

where C_i^r and D_i^r can be calculated as

$$C_i^r = \frac{\dfrac{P_k \rho_0}{\left(H^2 + \|\mathbf{q}_i - \mathbf{L}^r\|^2\right)^2} \log 2(e)}{\dfrac{\rho_0}{H^2 + \|\mathbf{q}_i - \mathbf{L}^r\|^2} \sum_{l=1}^{i} P_l + \sigma^2}, \tag{23}$$

$$D_i^r = \log_2\left(\frac{\rho_0}{H^2 + \|\mathbf{q}_i - \mathbf{L}^r\|^2} \sum_{l=1}^{i} P_l + \sigma^2\right). \tag{24}$$

With (19) and (22), (18b) can be transformed into

$$\tilde{R}_i^{[lb]} - \hat{R}_i \ge \eta_i. \tag{25}$$

(25) is still a non-convex constraint due to $\hat{R}_i$. Introducing $\mathbf{V} = \{V_i = \|\mathbf{q}_i - \mathbf{L}\|^2, \forall i\}$, $\hat{R}_i$ can be reformulated as

$$\hat{R}_i = \log_2\left(\frac{\rho_0}{H^2 + V_i} \sum_{k=1}^{i-1} P_k + \sigma^2\right), \tag{26}$$

where the slack variable needs to satisfy

$$V_i \le \|\mathbf{q}_i - \mathbf{L}\|^2, \forall i. \tag{27}$$

In (27), $\|\mathbf{q}_i - \mathbf{L}\|^2$ is convex with respect to $\mathbf{L}$, which can be approximated via Taylor expansion at the given point $\mathbf{L}^r$ as

$$\|\mathbf{q}_i - \mathbf{L}\|^2 \ge \|\mathbf{q}_i - \mathbf{L}^r\|^2 + 2\left(\mathbf{q}_i - \mathbf{L}^r\right)^{\mathrm{T}}\left(\mathbf{L} - \mathbf{L}^r\right). \tag{28}$$

Now, (26) can replace $\hat{R}_i$ in (25), which can be turned into

$$\tilde{R}_i^{[lb]} - \log_2\left(\frac{\rho_0}{H^2 + V_i} \sum_{k=1}^{i-1} P_k + \sigma^2\right) \ge \eta_i. \tag{29}$$

(29) is a convex constraint because it is jointly concave with respect to $\mathbf{L}^r$ and V_i.

For (18c), it can be regarded as $\tilde{R}_i$ with $i = 1$, which can be solved in a similar way. Thus, (18) can be made convex as

$$\max_{\mathbf{L},\mathbf{V}} \sum\nolimits_{i\in\mathcal{K}} \log_2\left(1 + \ \mathrm{SINR}_i\right) \tag{30a}$$

$$s.t. \begin{cases} \tilde{R}_i^{[lb]} - \log_2\left(\dfrac{\rho_0}{H^2 + V_i} \sum_{k=1}^{i-1} P_k + \sigma^2\right) \ge \eta_i, \\ \forall i \in \mathcal{K}\backslash\{1\}, \end{cases} \tag{30b}$$

$$V_i \le \|\mathbf{q}_i - \mathbf{L}^r\|^2 + 2\left(\mathbf{q}_i - \mathbf{L}^r\right)^{\mathrm{T}}\left(\mathbf{L} - \mathbf{L}^r\right), \tag{30c}$$

$$\tilde{R}_1^{[lb]} \ge \eta_1, \tag{30d}$$

which is convex and can be solved by CVX.

C. Iterative Algorithm

Based on Section III-A and Section III-B, (11) can be solved iteratively using Algorithm 1. In Step 3, the decoding order is updated according to the optimized UAV location.

Algorithm 1 Iterative Algorithm for (11)

Initialization: Set the geometric center of users as the starting location $\mathbf{L}^0 = \sum_{i=1}^{K} \mathbf{q}_i / K$. The initial decoding order and the power $\mathbf{P}^0$ are set according to $\mathbf{L}^0$ and the minimum transmit power. Set the initial index of iterations as $r = 0$.

while $(R(\mathbf{P}^{r+1}, \mathbf{L}^{r+1}) - R(\mathbf{P}^r, \mathbf{L}^r) \leq \epsilon_1)$ **do**

1. Solve (17) via $\mathbf{L}^r$, and obtain $\mathbf{P}^{r+1}$.
2. Solve (30) via $\mathbf{P}^{r+1}$, and obtain $\mathbf{L}^{r+1}$.
3. Update the decoding order according to $\mathbf{L}^{r+1}$.
4. Update: $r = r + 1$.

end

Output: $R_{sum}^* = R(\mathbf{P}^r, \mathbf{L}^r)$.

The convergence of Algorithm 1 is proved in Proposition 1.

Proposition 1: Algorithm 1 is convergent.

Proof: Define the objective value of rth iteration as $R(\mathbf{P}^r, \mathbf{L}^r)$. In the $(r+1)$th iteration, we obtain the objective value $R(\mathbf{P}^{r+1}, \mathbf{L}^r)$ by Step 1 of Algorithm 1, and it is the lower bound of the original problem (11). Thus we have

$$R(\mathbf{P}^r, \mathbf{L}^r) \leq R(\mathbf{P}^{r+1}, \mathbf{L}^r), \tag{31}$$

for Step 2 of Algorithm 1, and we can obtain the objective value $R(\mathbf{P}^{r+1}, \mathbf{L}^{r+1})$. Similarly, we have

$$R(\mathbf{P}^{r+1}, \mathbf{L}^r) \leq R(\mathbf{P}^{r+1}, \mathbf{L}^{r+1}). \tag{32}$$

Step 3 in Algorithm 1 can always adjust the current decoding order in each iteration, and the sum rate will not decrease. Thus, combining (31) with (32), we prove the objective value of (11) is non-decreasing after each iteration, and is upper bounded by a finite value. Algorithm 1 is convergent. ■

D. Analysis of the Last Decoding User

The last decoding user is the closest one to the UAV and last decoded via SIC. The last decoding user is determined when the UAV location is initialized, and will not change during iterations, which is proved in Proposition 2. To simplify the derivation, we introduce an auxiliary variable α_i as

$$\alpha_i = \frac{\sigma^2}{|h_i|^2}. \tag{33}$$

Proposition 2: The last decoding user is not changed during iterations and the optimal UAV location is getting closer to this user with increasing transmit power.

Proof: Define U_1 as the initial last decoding user, and we can always find suitable power allocation at $\mathbf{L}^0$ to satisfy

$$R_i(\alpha_i^*) = R_1(\alpha_1^*), \forall i \in \mathcal{K} \backslash \{1\}. \tag{34}$$

The derivative of $R_i(\alpha_i)$ and $R_1(\alpha_1)$ can be expressed as

$$\begin{aligned} R_i'(\alpha_i) &= (\log_2(1 + \text{SINR}_i(\alpha_i)))' \\ &= \frac{-P_i \log_2 e}{\left(\alpha_i + \sum\limits_{k=1}^{i-1} P_k\right)\left(\alpha_i + \sum\limits_{k=1}^{i} P_k\right)}, 2 \leq i \leq K, \end{aligned} \tag{35}$$

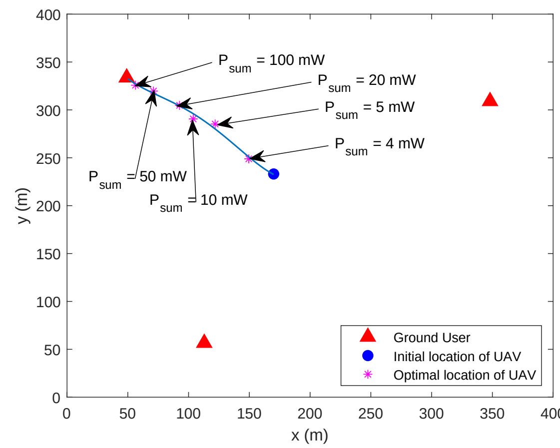

Fig. 1. The optimal UAV location with different values of P_{sum}. $\eta = (1, 1, 1)$ bit/s/Hz.

$$R_1'(\alpha_1) = \frac{-P_1 \log_2 e}{\alpha_1(\alpha_1 + P_1)}. \tag{36}$$

From (35) and (36), $R_i(\alpha_i)$ and $R_1(\alpha_1)$ decrease with α_i and α_1, respectively. To compare the first derivative values, we change the two functions into absolute values as

$$\begin{aligned} \frac{|R_i'(\alpha_i)|}{|R_1'(\alpha_1)|} &= \frac{P_i \alpha_1 (\alpha_1 + P_1)}{P_1 \left(\alpha_i + \sum\limits_{k=1}^{i-1} P_k\right)\left(\alpha_i + \sum\limits_{k=1}^{i} P_k\right)} \\ &= \frac{\text{SINR}_i(\alpha_i)(\alpha_1 + P_1)}{\text{SINR}_1(\alpha_1)\left(\alpha_i + \sum\limits_{k=1}^{i} P_k\right)}. \end{aligned} \tag{37}$$

According to the decoding order at $\mathbf{L}^0$, we have $h_1^* \geq h_i^*, i \in \mathcal{K}\backslash\{1\}$ and $\alpha_1^* \leq \alpha_i^*$. Thus, $|R_i'(\alpha_i^*)| < |R_1'(\alpha_1^*)|$ is met under the assumption in (34). In order to increase the sum rate, the UAV location will approach U_1. The user U_1 always has the best channel condition and the last decoding user is not changed. We can observe that the increase of power has a much greater influence on R_1 from (37). Therefore, with the rate thresholds are satisfied, the optimal UAV location will approach U_1 with larger P_{sum}. ■

From Proposition 2, we can conclude that the UAV location should move to the last decoding user, if we need to improve the sum rate with higher transmit power.

IV. Simulation Results and Discussion

In the simulation, assume that the UAV hovers at $H = 150$ m. We set $\sigma^2 = -110$ dBm and $\rho_0 = -60$ dB.

First, we set $K = 3$ and users are marked by red triangles, as shown in Fig. 1. The optimal location of UAV is presented for different transmit power, when $\eta = (1, 1, 1)$ bit/s/Hz. From the result, we can observe that the optimal UAV location becomes closer to the last decoding order when P_{sum} increases, which is consistent with the conclusion from Proposition 2.

The sum rate of the proposed scheme is compared in Fig. 2 with different η according to the topology in Fig. 1 with the same threshold for each user. The result shows that the sum rate increases when the transmit power of the UAV is higher.

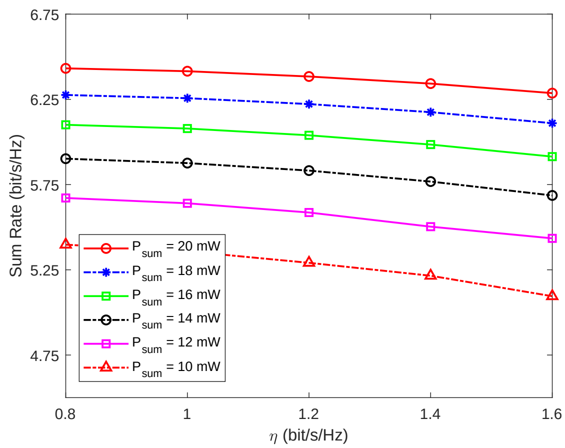

Fig. 2. Comparison of sum rate in the proposed scheme with different η, according to the topology in Fig. 1.

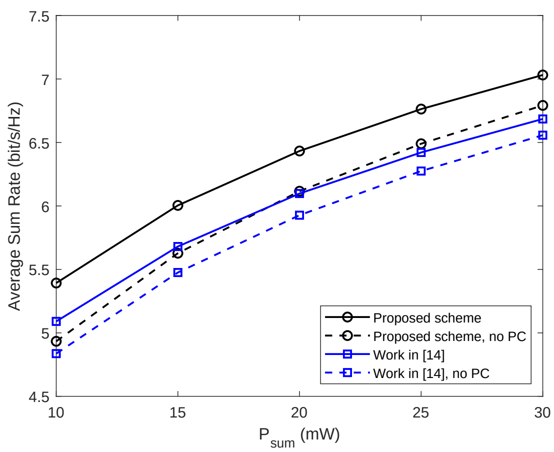

Fig. 3. Average sum rate comparison of the proposed scheme and the scheme in [14].

Furthermore, the sum rate decreases as the rate threshold increases. This is because that the lower threshold provides more degree of freedom for the power allocation and location selection, and thus the UAV can allocate more transmit power for the interference-free (last decoding) user, which leads to higher throughput.

In Fig. 3, the average sum rate of the proposed scheme is compared with the scheme in [14], with and without power control (PC). We assume all the users are randomly deployed in a square area of 400×400 m^2, and we set $\eta = (1, 1, 1)$ bit/s/Hz for all the schemes. The result shows PC can effectively improve the rate performance for both schemes. In addition, we can observe that the average sum rate of the proposed scheme is much higher than the benchmark scheme in [14]. For example, the average sum rate can be improved by 5% when $P_{sum} = 30$ mW.

V. Conclusions

In this letter, we have jointly optimized the UAV location and transmit power in NOMA-UAV networks via updating decoding order, which can be divided into two sub-problems. The non-convex sub-problems are approximated into convex ones, and an iterative algorithm is proposed to optimize the location and power alternately via successive convex optimization. Its convergence is proved. In addition, the closer performance of the algorithm has been further analyzed. Finally, simulation results have been shown to verify the effectiveness of the proposed scheme over benchmarks.

References

[1] Y. Zeng, R. Zhang, and T. J. Lim, "Wireless communications with unmanned aerial vehicles: Opportunities and challenges," *IEEE Commun. Mag.*, vol. 54, no. 5, pp. 36–42, May 2016.

[2] N. Zhao, W. Lu, M. Sheng, Y. Chen, J. Tang, F. R. Yu, and K. Wong, "UAV-assisted emergency networks in disasters," *IEEE Wireless Commun.*, vol. 26, no. 1, pp. 45–51, Feb. 2019.

[3] Q. Wu, Y. Zeng, and R. Zhang, "Joint trajectory and communication design for Multi-UAV enabled wireless networks," *IEEE Trans. Wireless Commun.*, vol. 17, no. 3, pp. 2109–2121, Mar. 2018.

[4] D. Yang, Q. Wu, Y. Zeng, and R. Zhang, "Energy tradeoff in ground-to-UAV communication via trajectory design," *IEEE Trans. Veh. Technol.*, vol. 67, no. 7, pp. 6721–6726, Jul. 2018.

[5] J. Zhao, F. Gao, L. Kuang, Q. Wu, and W. Jia, "Channel tracking with flight control system for UAV mmwave MIMO communications," *IEEE Commun. Lett.*, vol. 22, no. 6, pp. 1224–1227, Jun. 2018.

[6] S. Gong, S. Wang, C. Xing, S. Ma, and T. Q. S. Quek, "Robust superimposed training optimization for UAV assisted communication systems," *IEEE Trans. Commun.*, vol. 19, no. 3, pp. 1704–1721, Mar. 2020.

[7] C. O. Nnamani, M. R. A. Khandaker, and M. Sellathurai, "UAV-aided jamming for secure ground communication with unknown eavesdropper location," *IEEE Access*, vol. 8, pp. 72 881–72 892, Apr. 2020.

[8] Z. Chen, Z. Ding, X. Dai, and R. Zhang, "An optimization perspective of the superiority of NOMA compared to conventional OMA," *IEEE Trans. Signal Process.*, vol. 65, no. 19, pp. 5191–5202, Jul. 2017.

[9] Z. Chang, L. Lei, H. Zhang, T. Ristaniemi, S. Chatzinotas, B. Ottersten, and Z. Han, "Energy-efficient and secure resource allocation for multiple-antenna NOMA with wireless power transfer," *IEEE Trans. on Green Commun. Netw.*, vol. 2, no. 4, pp. 1059–1071, Dec. 2018.

[10] H. Lei, J. Zhang, K. Park, P. Xu, Z. Zhang, G. Pan, and M. Alouini, "Secrecy outage of max-min TAS scheme in MIMO-NOMA systems," *IEEE Trans. Veh. Technol.*, vol. 67, no. 8, pp. 6981–6990, Aug. 2018.

[11] Y. Liu, Z. Qin, Y. Cai, Y. Gao, G. Y. Li, and A. Nallanathan, "UAV communications based on non-orthogonal multiple access," *IEEE Wireless Commun.*, vol. 26, no. 1, pp. 52–57, Feb. 2019.

[12] W. Mei and R. Zhang, "Uplink cooperative NOMA for cellular-connected UAV," *IEEE J. Sel. Topics Signal Proc.*, vol. 13, no. 3, pp. 644–656, Jun. 2019.

[13] R. Tang, J. Cheng, and Z. Cao, "Joint placement design, admission control, and power allocation for NOMA-based UAV systems," *IEEE Wireless Commun. Lett.*, vol. 9, no. 3, pp. 385–388, Mar. 2020.

[14] X. Liu, J. Wang, N. Zhao, Y. Chen, S. Zhang, Z. Ding, and F. R. Yu, "Placement and power allocation for NOMA-UAV networks," *IEEE Wireless Commun. Lett.*, vol. 8, no. 3, pp. 965–968, Mar. 2019.

[15] A. A. Nasir, H. D. Tuan, T. Q. Duong, and H. V. Poor, "UAV-enabled communication using NOMA," *IEEE Trans. Commun.*, vol. 67, no. 7, pp. 5126–5138, Jul. 2019.

[16] M. Liu, J. Yang, and G. Gui, "DSF-NOMA: Uav-assisted emergency communication technology in a heterogeneous internet of things," *IEEE Internet Things J.*, vol. 6, no. 3, pp. 5508–5519, Jun. 2019.

[17] W. Wang, J. Tang, N. Zhao, X. Liu, X. Zhang, Y. Chen, and Y. Qian, "Joint precoding optimization for secure SWIPT in UAV-aided NOMA networks," *IEEE Trans. Commun.*, vol. 68, no. 8, pp. 5028–5040, Aug. 2020.

[18] Y. Li, H. Zhang, K. Long, S. Choi, and A. Nallanathan, "Resource allocation for optimizing energy efficiency in NOMA-based fog UAV wireless networks," *IEEE Network*, vol. 34, no. 2, pp. 158–163, Mar. 2020.

[19] X. Pang, J. Tang, N. Zhao, X. Y. Zhang, and Y. Qian, "Energy-efficient design for mmwave-enabled NOMA-UAV networks," *Sci. China Inf. Sci.*, Online. DOI: 10.1007/s11432-020-2985-8.

[20] C. Pan, H. Ren, Y. Deng, M. Elkashlan, and A. Nallanathan, "Joint blocklength and location optimization for URLLC-enabled UAV relay systems," *IEEE Commun. Lett.*, vol. 23, no. 3, pp. 498–501, Mar. 2019.